The oldest fossil record of the extant penguin genus *Spheniscus*—a new species from the Miocene of Peru

URSULA B. GÖHLICH

Göhlich, U.B. 2007. The oldest fossil record of the extant penguin genus *Spheniscus*—a new species from the Miocene of Peru. *Acta Palaeontologica Polonica* 52 (2): 285–298.

Described here is a partial postcranial skeleton and additional disarticulated but associated bones of the new fossil penguin *Spheniscus muizoni* sp. nov. from the latest middle/earliest late Miocene (11–13 Ma) locality of Cerro la Bruja in the Pisco Formation, Peru. This fossil species can be attributed to the extant genus *Spheniscus* by postcranial morphology and is the oldest known record of this genus. *Spheniscus muizoni* sp. nov. is about the size of the extant Jackass and Magellanic penguins (*Spheniscus demersus* and *Spheniscus magellanicus*). Beside *Spheniscus urbinai* and *Spheniscus megaramphus* it is the third species of *Spheniscus* represented in the Pisco Formation. This study contains morphological comparisons with Tertiary penguins of South America and with most of the extant penguin species.

Key words: Spheniscidae, Pisco Formation, Miocene, Peru.

Ursula B. Göhlich [ursula.goehlich@nhm-wien.ac.at], Université Claude Bernard – Lyon 1, UMR P.E.P.S., Bâtiment Géode, 2 rue Dubois, F-69622 Villeurbanne Cedex, France; present address: Naturhistorisches Museum Wien, Geologisch-Paläontologische Abteilung, Burgring 7, A-1010 Wien, Austria.

Introduction

The fossil record of penguins in South America comes from both Atlantic and Pacific coasts and is restricted to findings in Argentina, Chile, and Peru; their stratigraphic distribution ranges from the late Eocene?–early Oligocene (Acosta Hospitaleche 2005) to the late Pliocene (Emslie and Correa 2003). Most of the described fossil species come from the early Miocene of Patagonia, Argentina (see Ameghino 1891, 1895, 1899, 1901, 1905, 1920; Moreno and Mercerat 1891; Simpson 1972, 1975a). Recently, the South American fossil penguins have been taxonomically revised (e.g., Acosta Hospitaleche 2003, 2005; Acosta Hospitaleche and Canto 2005; Acosta Hospitaleche and Tambussi 2004a, b; Acosta Hospitaleche et al. 2005) and concluded in a reduction of 35 formerly named penguin species to about 14 different taxa, which are exclusive to South America (Acosta Hospitaleche and Tambussi 2004a, b). The following taxa are known from Argentina: *Arthrodytes andrewsi* (Ameghino, 1901) and *Paraptenodytes robustus* (Ameghino, 1895) (both from the upper Eocene–lower Oligocene San Julian Formation, Patagonia), *Eretiscus tonnii* (Simpson, 1981), *Palaeospheniscus bergi* Moreno and Mercerat, 1891, *Ps. patagonicus* Moreno and Mercerat, 1891, *Ps. biloculata* Simpson, 1970 (all from the lower Miocene Gaiman Formation, Patagonia), *Paraptenodytes antarcticus* (Moreno and Mercerat, 1891) (from the lower Miocene Monte Léon Formation and the lower upper Miocene Puerto Madryn Formation, both Patagonia) and *Madrynornis mirandus* Acosta Hospitaleche, Tambussi, Donato, and Cozzuol, 2007 (this volume; from the lower upper Miocene Puerto Madryn Formation, Patagonia). The Chilean fossil penguin taxa include: *Paraptenodytes robustus*, *Pa. antarcticus*, *Palaeospheniscus* sp., *Pygoscelis grandis* Walsh and Suárez, 2006, *Py. caldernensis* Acosta Hospitaleche, Chávez, and Fritis, 2006, *Spheniscus* sp. (all from the upper Miocene–lower Pliocene, Bahia Inglesa Formation), and *Spheniscus chilensis* Emslie and Correa, 2003 (late Pliocene, Mejillones Formation). The following taxa are known from Peru: a Spheniscidae indet. (late Eocene–early Oligocene, Otuma Formation), *Palaeospheniscus* sp. (lower middle Miocene, Chilcatay Formation), *Spheniscus urbinai* Stucchi, 2002 and *S. megaramphus* Stucchi, Urbina, and Giraldo, 2003 (both from the upper Miocene–lower Pliocene of the Pisco Formation).

Thus, findings of fossil representatives of the extant penguin genus *Spheniscus* are restricted to Peru and Chile and have been known from the late Miocene to late Pliocene hitherto. For the Pisco Formation of Peru, Noriega and Tambussi (1989) and Cheneval (1993) already mentioned probable new taxa of Spheniscidae, but did not name them; recently they have been described by Stucchi (2002) and Stucchi et al. (2003) as *Spheniscus urbinai* from different sites of late Miocene to early Pliocene age and as *S. megaramphus* from the upper Miocene of the Montemar locality. In Chile, fossils of *Spheniscus* are described as cf. *Spheniscus* by Walsh and Hume (2001) from the middle Miocene–lower Pliocene Bahía Inglesa Formation and as *S. chilensis* Emslie and Correa, 2003 from the late Pliocene (Mejillones Formation) of Cuenca del Tiburón, Península de Mejillones.

Herein a new fossil species of *Spheniscus* is described again from the Pisco Formation in Peru, but coming from older deposits at the Cerro la Bruja locality of latest middle/earliest late Miocene (11–13 Ma) age.

Institutional abbreviations.—LACM, Natural History Museum of Los Angeles County, Los Angeles, USA; MNHN, Muséum National d'Histoire Naturelle, Paris, France; SAPM, Staatssammlung für Anthropologie und Paläoanatomie, Munich, Germany; UCBL, Université Claude Bernard, Lyon 1, France; UF, University of Florida, Florida Museum of Natural History, USA.

Geological setting

The locality of Cerro la Bruja, Department of Ica, is situated in the marine Pisco Formation (Fig. 1). The age of the Pisco Formation ranges from the middle Miocene to early Pliocene (Muizon and DeVries 1985). The deposit of Cerro la Bruja is dated on biostratigraphic data to be of latest middle Miocene to earliest late Miocene age (13–11 Ma; Muizon 1988), and therefore represents the oldest deposit within the Pisco Formation.

The Pisco Formation corresponds to a marine transgression along the southern coast of Peru during the Neogene and is known for its abundant marine vertebrate fauna. Its geology and palaeoecology in the Sacaco area were studied by Muizon and DeVries (1985). The marine bird fauna is one of the richest known from the Neogene of South America. Beside Cerro la Bruja other fossil penguin bearing localities in the Pisco Formation are: El Jahuay (ELJ), ca. 9 Ma, late Miocene; Aguada de Lomas (AGL), ca. 7–8 Ma (Muizon et al. 2003), late Miocene; Montemar (MTM), ca. 6 Ma, late Miocene; Sacaco Sud (SAS), ca. 5 Ma, early Pliocene; Sacaco (SAO), ca. 3.5 Ma, early Pliocene (datings from Muizon 1984, 1988; Muizon and DeVries 1985). For additional vertebrate faunas see Conclusions.

Material and methods

The osteological terminology used here follows Baumel et al. (1993) but terms are translated into English. Measurements were taken after von den Driesch (1976) and Stephan (1979). For metrical comparisons, using published data, it has to be considered that different authors (e.g., Simpson 1946, 1975b, 1979a, b), had slightly deviating ways of measuring the greatest lengths of some limb bones; often they measured the functional lengths, taking recessed points or sulci between condyles (e.g., for femur, distal tibiotarsus, distal tarsometatarsus) as landmarks. However, the differences in the values are never more than a few mm.

The penguin material of Cerro la Bruja described here comes from excavations of Christian de Muizon and belongs to MNHN, but is temporarily housed in the collections of UCBL. For morphological comparisons with the fossil Chilean species, *Spheniscus chilensis,* parts of the paratype material (UF 143295, 143299, 144112, 144134, 144148, 144149, 144154, 144168, 144169) were at disposal by loan. Morphological comparisons with extant penguins are based on following specimens provided by the collections of SAPM and UCBL: *Spheniscus humboldti* (SAPM 5 ♂, 12 ♀; UCBL 25588), *S. demersus* (SAPM 12 ♂, 13 ♀), *S. magellanicus* (SAPM 8 ♂, 9 ♀), *Eudyptes chrysochome* (junior synonym *E. crestatus*), (SAPM 6 ♂, 5 ♀), *E. chrysolophus* (SAPM 1 ?), *Aptenodytes patagonicus* (SAPM 6 ♂, 8 ♀), *Pygoscelis papua* (SAPM 12 ♂, 3 ♀), and *Py. adeliae* (UCBL XII 1978). Metric data of extant penguin species were acquired on the aforementioned specimens as well as additional material from the SAPM. Measurements of *S. mendiculus* are based on specimens at the LACM and were provided by Kenneth Campbell.

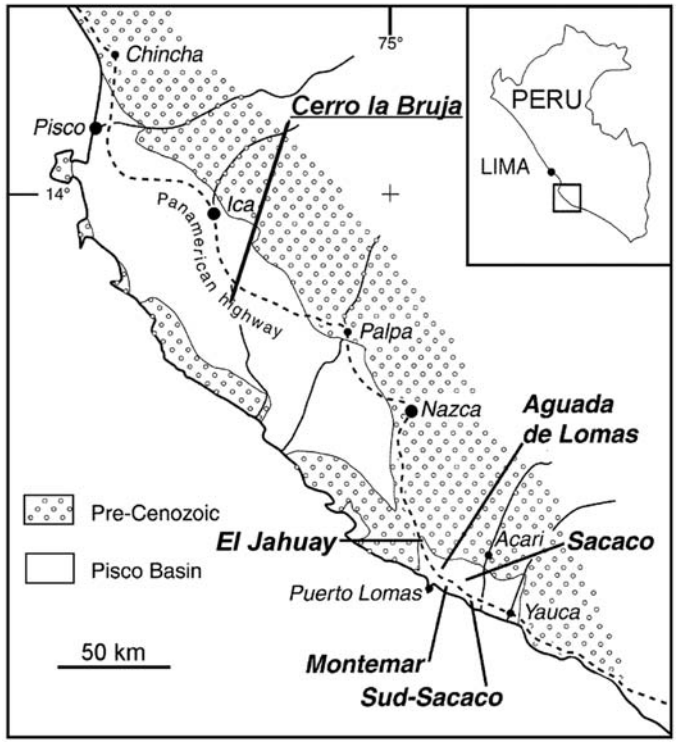

Fig. 1. Geographic position of the latest middle/earliest late Miocene locality Cerro La Bruja, and further fossil penguin bearing localities in the Pisco Formation, Peru. Modified after McDonald and Muizon (2002: fig. 1).

Systematic palaeontology

Sphenisciformes Sharpe, 1891

Spheniscidae Bonaparte, 1831

Genus *Spheniscus* Moehring, 1758

Type species: *Spheniscus demersus* (Linnaeus, 1758).

Remarks.—Based on the following osteological features the postcranial penguin material of Cerro la Bruja, presented here, can be affiliated to *Spheniscus* on generic level.

Humerus with humeral head barely swollen proximally (more swollen in *Aptenodytes*, *Pygoscelis*, and *Eudyptes*), proximal outline of humerus without proximal notch between

dorsal tubercle and the head (notched in *Aptenodytes*, *Pygoscelis*, and *Eudyptes*, slightly notched in *Palaeospheniscus*); bipartite pneumotricipital fossa with a deep cranial fossa (non-bipartite in *Paraptenodytes* and *Arthrodytes*); proximal border of pneumotricipital fossa in ventral view straight and almost horizontally (proximally concave in *Aptenodytes* and *Eudyptes*); caudal-most process of the ventral epicondyle hardly surpassing ventral margin of distal humerus shaft (in cranial/caudal view; clearly surpassing in *Aptenodytes* and *Pygoscelis*). Coracoid with probably closed supracoracoid foramen (open in *Pygoscelis*, *Eudyptula*, and *Aptenodytes* and probably in *Palaeospheniscus*). Femoral head and trochanter proximally at same level (trochanter higher in *Eudyptes*, *Pygoscelis*, and *Aptenodytes*). Tarsometatarsus quite elongate, with an elongation index (maximal length/proximal width) of 2.07, thus smaller than in *Palaeospheniscus* (elongation index: 2.2–2.4); extensor sulci long and deep (shallower in *Eudyptes*, *Pygoscelis*, and *Aptenodytes*); trochlea II and trochlea IV of about same length distally (unlike in *Palaeospheniscus*, *Eudyptes*, *Pygoscelis*, and *Aptenodytes*, where trochlea IV is somewhat shorter than trochlea II); the position and arrangement of the two proximal vascular foramina and of the very pronounced impressions of the extensor retinaculum corresponds best with *Spheniscus*; lateral intertrochlear incision deeper incised proximally than medial one.

Spheniscus muizoni sp. nov.

Figs. 2, 3, 4A, C, E, G, I, 5A.

Holotype: Partial postcranial skeleton MNHN PPI 147: subcomplete left and right coracoid (147a); cranial end of left and subcomplete right scapula (147b); subcomplete left and right humerus (147c); left complete ulna (147d); proximal and distal end of right femur (147e); complete right and proximal end of left tibiotarsus (147f); proximal end of left fibula (147g); right complete tarsometatarsus (147h), cranial portion of sternum with articular sulcus for coracoid and fragment of the craniolateral process (147i); two fragmentary thoracic vertebrae (147j) from the caudal region; seven caudal vertebrae (147k); fragmentary synsacrum (147l);

Paratypes: Additional isolated bones from the type locality (MNHN PPI 148–153): distal fragmentary half of left coracoid, worn (148); right subcomplete coracoid (155); left complete ulna (149); left complete radius (150); right complete carpometacarpus (154); distal end of right femur (151); cranial end of pygostyle (152); rib fragment without ends (153).

Derivation of the name: Named after Christian de Muizon (MNHN) who collected the studied material and graciously placed it at my disposal; and in recognition of his efforts and paleontological investigations on the vertebrate fauna of the Pisco Formation in Peru.

Type locality and horizon: Cerro la Bruja, Department of Ica, Peru; Pisco Formation, latest middle/earliest late Miocene, ca. 13–11 Ma (Muizon 1988).

Diagnosis.—Small-sized fossil Spheniscidae; similar in size to extant *Spheniscus magellanicus* (Forster, 1781) and *S. demersus* (Linnaeus, 1758), slightly smaller than *S. humboldti* Meyen, 1834, but lager than *S. mendiculus* Sundevall, 1871. Distinctly smaller than the fossil species *S. urbinai* and *S. megaramphus*, but of similar size to *S. chilensis* (Tables 1, 2 and Fig. 6).

Carpometacarpus with distinct step between the proximal carpal trochlea and the extensor process of the alular metacarpal (step weaker or absent in extant species of *Spheniscus*), an almost complete fusion of proximal alular digit with the major metacarpal (fusion less advanced in *S. chilensis*), and an open spatium without ossified synchondroses (unlike *S. chilensis* with synchondroses).

Humerus with humeral head barely swollen proximally, proximal outline without proximal notch between dorsal tuberculum and the head, but proximal outline less steep (in caudal view) than in all compared extant species of *Spheniscus*; proximal border of pneumotricipital fossa forms no ventrocaudally projecting lip, a feature shared with *S. urbinai* and *S. chilensis*, but unlike in extant species of *Spheniscus* and *Pygoscelis*; proximal border of pneumotricipital fossa in ventral view straight and almost horizontally like in extant *Spheniscus* species (unlike in *S. chilensis*, *S. urbinai*, *Dege hendeyi*, and extant species of *Aptenodytes* and *Eudyptes* where it is proximally concave); distinct concave indentation of bicipital crest between ventral tuberculum and shaft, but which is absent in *S. chilensis*; preaxial angle situated more proximally than in other penguin taxa, at about mid of shaft length; caudal-most tip at the ventral epicondylus (process-like crest caudally bordering the humerotricipital sulcus) slightly oriented upwards (ventroproximally); cranial-most tip at ventral epicondylus (process-like crest caudally bordering the scapulotricipital sulcus) projecting ventrodistally somewhat longer and oriented slightly more distally than in *S. chilensis*.

Femoral head and trochanter at about the same level proximally; medial condyle cranially very low and hardly projecting (unlike in all other compared extant and fossil penguins), lateral condyle prominent and reaching further proximally than medial one.

Tibiotarsus characterized by its straight (not medially deflected) and relatively narrow (in cranial/caudal view) distal end; distinct and deep medial impression of the medial collateral ligament situated mediocaudally on proximal end.

Tarsometatarsus quite elongate and slender; proximal end relatively narrow; elongation index (2.07) higher than in *S. urbinai*, but smaller than in *Palaeospheniscus*; extensor sulci long and deep; extremely deep dorsal infracotylar fossa; proximal vascular foramina on different level (same level in *Palaeospheniscus*), medial proximal vascular foramen small and situated very proximomedially; hypotarsus with medial hypotarsal crest oriented medioplantarly and bent medially; medial hypotarsal crest divided in two crests, with lateral one being very weak, thin, and shorter; lateral hypotarsal crest blunt and low; lateral intertrochlear incision longer proximally than medial one; trochlea II and IV of about same length distally (unlike in *Palaeospheniscus*); lateral condyle of trochlea III (in distal view) at same level dorsally as trochlea IV (plantarly recessed in extant *Spheniscus* and *S. chilensis*); lateral and medial condyle of trochlea III (in distal view) dorsally at about same (medial one dorsally more swollen in extant *Spheniscus* and *S. urbinai*); trochlea

Table 1. Measurements of *Spheniscus muizoni* sp. nov. from Cerro la Bruja in the Pisco Formation; n, number of specimens; parentheses indicate estimated values.

Skeletal elements and measured sections	Measurements (mm)	n
scapula		
greatest length	–	–
maximal diagonal cranial end	20.4	1
smallest width of neck	10.9	2
coracoid		
greatest length (medial)	76.3–79.4	2
length, lateral	76.3	1
width, distal	23.9	1
width of distal facies	23.7	1
smallest width of shaft, including foramen nervi supracoracoidei	11.9–14.4	4
humerus		
greatest length including ventral epicondylus	74.0	1
length (from head to condylus ventralis)	69.6–70.9	2
greatest width of proximal end	22.6–22.9	2
greatest depth of proximal end	15.0–15.6	2
smallest width of shaft	13.1–13.4	2
greatest diagonal width of distal end	24.0	1
ulna		
greatest length	50.2–50.5	2
depth of proximal facies articularis	(7.1)	1
greatest width of shaft	17.7	1
greatest diagonal of distal end	7.1–8.2	2
radius		
greatest length	47.7	1
depth of proximal facies articularis	5.6	1
width of proximal end	(8.1)	1
greatest width of shaft	11.6	1
diagonal of distal facies articularis	6.6	1
carpometacarpus		
greatest length	41.0	1
length (of metacarpale majus)	39.4	1
width of proximal end	14.8	1
maximal width of body	15.6	1
diagonal width of distal facies articularis	12.5	1

Skeletal elements and measured sections	Measurements (mm)	n
femur		
greatest length	–	–
width of proximal end	17.6	1
depth of proximal end	11.9	1
smallest width of body	–	–
width of distal end	(15.5)–16.1	2
depth of distal end	15.4–15.7	2
tibiotarsus		
greatest length (including crista cnemialis cranialis)	110.6	1
length (from area interarticularis to distalmost point of distal end)	106.9	1
greatest diagonal of proximal end	(17.5)–(18.1)	2
width of proximal end	11.4–12.2	2
smallest width of body	8.5	1
greatest width of distal end	14.5	1
greatest depth of distal end	15.1	1
fibula		
greatest length	–	–
width of proximal end	(7.7)	1
depth of proximal end	(4.4)	1
tarsometatarsus		
greatest length (from eminentia intercotylaris to distal most point of trochlea III)	33.7	1
width, proximal	16.3	1
depth, proximal with hypotarsus	10.5	1
smallest width of body	15.0	1
width of distal end	21.6	1
ratio length / minimal width of shaft	2.25	1
ratio length / maximal width of proximal end	2.07	1
pygostyl		
greatest length	–	–
greatest width	6.1	1
greatest height	12.3	1

II oriented somewhat obliquely; lateral condyle of trochlea IV (in distal view) plantarly tapering.

Description and comparisons

Remarks.—For measurements of *Spheniscus muizoni* sp. nov. see Table 1. The material represents bones of at least two individuals. None of the bones provides any indication that the studied individuals of the new species are juveniles. No cranial material is preserved; for this reason comparisons with *S. megaramphus* are impossible, which is only known by its skull and mandible. However, *S. muizoni* sp. nov. is distinctly smaller than both *S. megaramphus* and *S. urbinai* (Fig. 6). In the following, comparisons are priorly made with both extant and fossil species of *Spheniscus*, but also with extant taxa, with fossil South American taxa (*Palaeospheniscus*, *Paraptenodytes*, *Arthrodytes*, and *Eretiscus*), and subordinate with the South African fossil taxa (*Nucleornis*, *Dege*, *Inguza*, and ?*Palaeospheniscus huxleyorum*), because the later are supposed to be closely related with *Spheniscus* by Olson (1985: 151).

Scapula (Fig. 2A).—Two fragmentary scapulae, a cranial end of a left scapula and a damaged cranial half of a right scapula, lacking most of the cranial end, are preserved (MNHN PPI 147b1-2). In cranial view, the cranial end is mediolaterally narrow; specifically the ventral part is slightly narrower than in *S. humboldti* and *S. demersus*, and more closely resembling *S. magellanicus*. The coracoid tubercle is elliptical and also mediolaterally narrow. The acromion is broken off in both specimens (which is of different length and direction within extant genera). Medially on the cranial end, a distinct but low crest runs from the acromion diagonally ventrocaudally to below the coracoid tubercle; such a distinct crest could not be observed in any of the compared

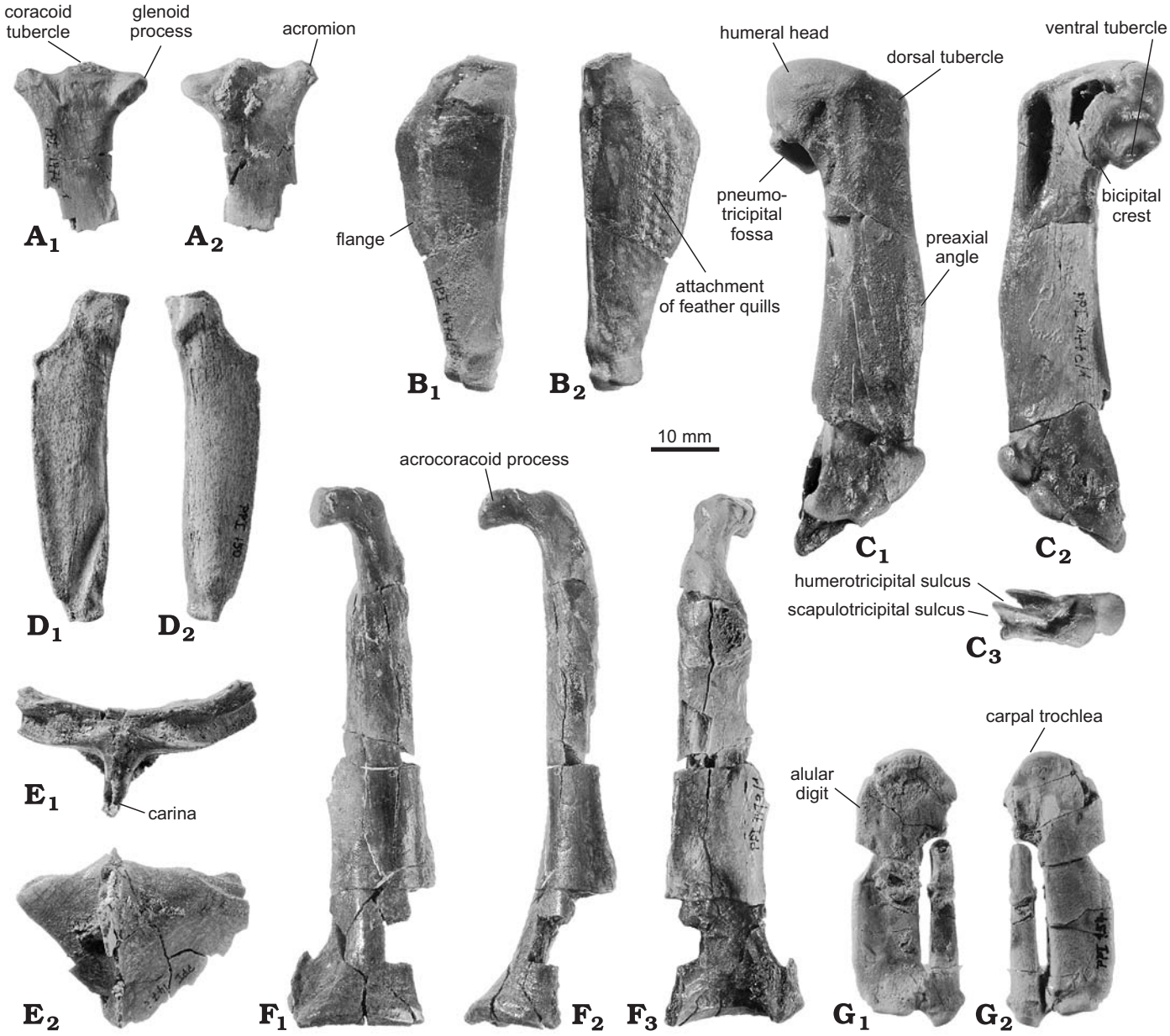

Fig. 2. Spheniscid penguin *Spheniscus muizoni* sp. nov. from Cerro la Bruja, latest middle/earliest late Miocene, Pisco Formation, Peru. **A**. Left scapula (MNHN PPI 147b) cranial end, in medial (A_1) and lateral (A_2) views. **B**. Left ulna (MNHN PPI 147d), in ventral (B_1) and dorsal (B_2) views. **C**. Left humerus (MNHN PPI 147c), in caudal (C_1), cranial (C_2), and distal (C_3) views. **D**. Left radius (MNHN PPI 150), in dorsal (D_1) and ventral (D_2) views. **E**. Cranial portion of sternum (MNHN PPI 147i), in cranial (E_1) and ventral (E_2) views. **F**. Left coracoid (MNHN PPI 147a), in ventral (F_1), ventrolateral (F_2), and dorsal (F_3) views. **G**. Right carpometacarpus (MNHN PPI 154), in ventral (G_1) and dorsal (G_2) views.

extant penguin taxa. The glenoid process is mediodistally oblate. The medial articular facet for the coracoid on the glenoid process is bordered medially and ventrally by a weak edge. The collum is quite mediolaterally flattened; the ventral margin of the scapular blade carries a little projection about 20 mm caudally the cranial end.

Coracoid (Fig. 2F).—Fragmentary left and right coracoid of the partial skeleton (MNHN PPI 147a/1-2) and a distal fragmentary half of a worn left coracoid (MNHN PPI 148) are present. The left coracoid lacks the procoracoid process and the lateral angle of the distal end, the right one lacks the proximal end. The coracoid corresponds well with the morphology of the extant species of *Spheniscus* and of *S. urbinai* and *S. chilensis*. The acrocoracoid process is long and angled rectangular to the bone; its distal margin is almost straight in dorsal/ventral view. In proximal view, the ventral inflexion of the procoracoid process is a little less close than in the extant species of *Spheniscus*. The scapular cotyla is round and relatively large; the articular facet for the humerus is oval and flat and not well defined. Despite the procoracoid process is lacking in both specimens, the fracture at the right coracoid

Table 2. Metrical comparisons of *Spheniscus muizoni* sp. nov. with the fossil species and most extant species of *Spheniscus* and all Tertiary penguin species from South Africa. Own measurements for *S. muizoni*, *S. urbinai*, *S. magellanicus*, *S. demersus*, *S. humboldti*. Measurements of *S. chilensis* provided by Steve Emslie and own measurements. Measurements of *S. mendiculus* from Emslie and Correa (2003), of *Nucleornis insolitus* from Simpson (1979a), of *Inguza predemersus* from Simpson (1975a, Bp and KC were measured from fig. 4 in Simpson 1975a), of *Dege hendeyi* from Simpson (1979b), and of *Palaeospheniscus huxleyorum* from Simpson (1973). L, length; GL, greatest length; Bp, breadth, proximal; KC, smallest width of body; $\bar{x}$, mean; n, number of specimens; log values explained and used in Fig. 6.

Skeletal elements and measured sections		*Spheniscus muizoni* sp. nov.				*Spheniscus urbinai*				*Spheniscus chilensis*			
		min.–max.	$\bar{x}$	n	log	min.–max.	$\bar{x}$	n	log	min.–max.	$\bar{x}$	n	log
humerus	L	69.6–70.9	70.3	2	–0.07	85.9–108	99.2	42	0.142	68.2–72.2	70.2	5	–0.008
ulna	GL	50.2–50.5	50.3	2	–0.024	(60.4)–79.8	72.9	28	0.138	48.4–54.3	51.0	3	–0.018
carpometacarpus	GL	41.0	–	1	–0.025	54.7–67.1	61.6	24	0.152	42.0–45.9	44.4	4	0.010
femur	GL	–	–	–	–	(106)–130.5	116.5	26	0.150	78	78	1	–0.024
tibiotarsus	L	106.9	–	1	–0.029	(133)–166	148.3	20	0.113	–	–	–	–
tarsometatarsus	GL	33.7	–	1	–0.014	(41)–52.2	45.6	28	0.117	33.5	33.5	2	–0.017
	Bp	16.3	–	1	–	21.9–28.1	24.5	23	–	–	–	–	–
	KC	15	–	1	–	(15)–22.4	23.0	30	–	16	16	2	–
ratio GL/Bp		2.07	–	–	–	1.72–1.95	1.85	19	–	–	–	–	–
ratio GL/KC		2.24	–	–	–	1.76–2.18	1.96	21	–	2.09	–	1	–
		Spheniscus magellanicus				*Spheniscus demersus*				*Spheniscus humboldti*			
humerus	L	65.3–73.2	69.3	6	–0.014	62.0–73.6	66.9	16	–0.029	68.6–74.3	71.5	13	–
ulna	GL	46.5–54.9	50	6	–0.026	46.5–53.8	49.9	16	–0.027	51.3–56.2	53.1	13	–
carpometacarpus	GL	39.2–44.2	41.8	6	–0.016	38.5–44.1	41.2	16	–0.023	40.8–45.6	43.4	13	–
femur	GL	72.4–84.4	77.9	6	–0.024	64.3–85.0	73.5	16	–0.050	78.0–86.3	82.4	13	–
tibiotarsus	L	101.5–118.9	110.3	6	–0.015	92.4–119.8	105.6	15	–0.034	107.1–119.7	114.3	13	–
tarsometatarsus	GL	30.7–35.5	33.4	6	–0.018	29.2–35.4	32.4	16	–0.031	33.1–37.2	34.8	13	–
		Spheniscus mendiculus				*Nucleornis insolitus*				*Inguza predemersus*			
humerus	L	56.0–58.8	57.0	3	–	–	–	–	–	57.5–59.0	58.3	2	–0.089
ulna	GL	–	–	–	–	–	–	–	–	–	–	–	–
carpometacarpus	GL	–	–	–	–	–	–	–	–	–	–	–	–
femur	GL	–	–	–	–	–	–	–	–	59.8–62.3	61.2	3	–0.129
tibiotarsus	L	–	–	–	–	–	–	–	–	85.2–92.0	–	2	–0.111
tarsometatarsus	GL	–	–	–	–	40.4	–	1	0.065	27.2	27.2	1	–0.107
	Bp	–	–	–	–		–	–	–	12.8	–	–	–
	KC	–	–	–	–	21.6	–	–	–	12	–	–	–
ratio GL/Bp		–	–	–	–	–	–	–	–	2.13	–	–	–
ratio GL/KC		–	–	–	–	1.87	–	–	–	2.27	–	–	–
		Dege hendeyi				?*Palaeospheniscus huxleyorum*							
humerus	L	68.5–69	68.8	2	–0.017	ca. 63	–	1	–0.055				
ulna	GL	–	–	–	–	–	–	–	–				
carpometacarpus	GL	–	–	–	–	–	–	–	–				
femur	GL	70.4–79.5	75.1	6	–0.04	–	–	–	–				
tibiotarsus	L	106.5–108.2	107.9	2	–0.025	–	–	–	–				
tarsometatarsus	GL	–	–	–	–	–	–	–	–				

indicates a closed supracoracoid foramen as in all extant *Spheniscus*; its length can be estimated as about 6 mm. There is no osteological indication if there was a second foramen, larger and distally to the first one, as often developed in extant *Spheniscus*; however, its presence or absence can vary intraspecifically, following own observations. The distal end of the coracoid is dorsally strongly concave; the lateral process is short and thin, and forms laterally a concave margin. The medial angle is thickened, proximodistally elongated and forms a pin-like process in proximal direction. Ventral to the medial angle, the surface of the coracoid forms a concavity. The articular facet for the sternum is separated from the medial angle by a little indentation on the distal margin.

The coracoid of *Spheniscus muizoni* sp. nov. distinguishes from the fragmentary preserved coracoid of *S. chilensis* (Emslie and Correa 2003: fig. 2B) only by a somewhat shorter supracoracoid foramen. However, its length is variable in extant *Spheniscus* species and therefore probably not diagnostic.

The closed supracoracoid foramen distinguishes *S. muizoni* sp. nov. from *Palaeospheniscus*, in which it is open, as suggested by Simpson (1946: 49). In contrary to *Ps. patagonicus* and *Ps. bergi* (figured in Moreno and Mercerat 1891: pl. 1: 23, 25), the coracoid of *S. muizoni* sp. nov. is smaller and more slender, especially at the level of the foramen.

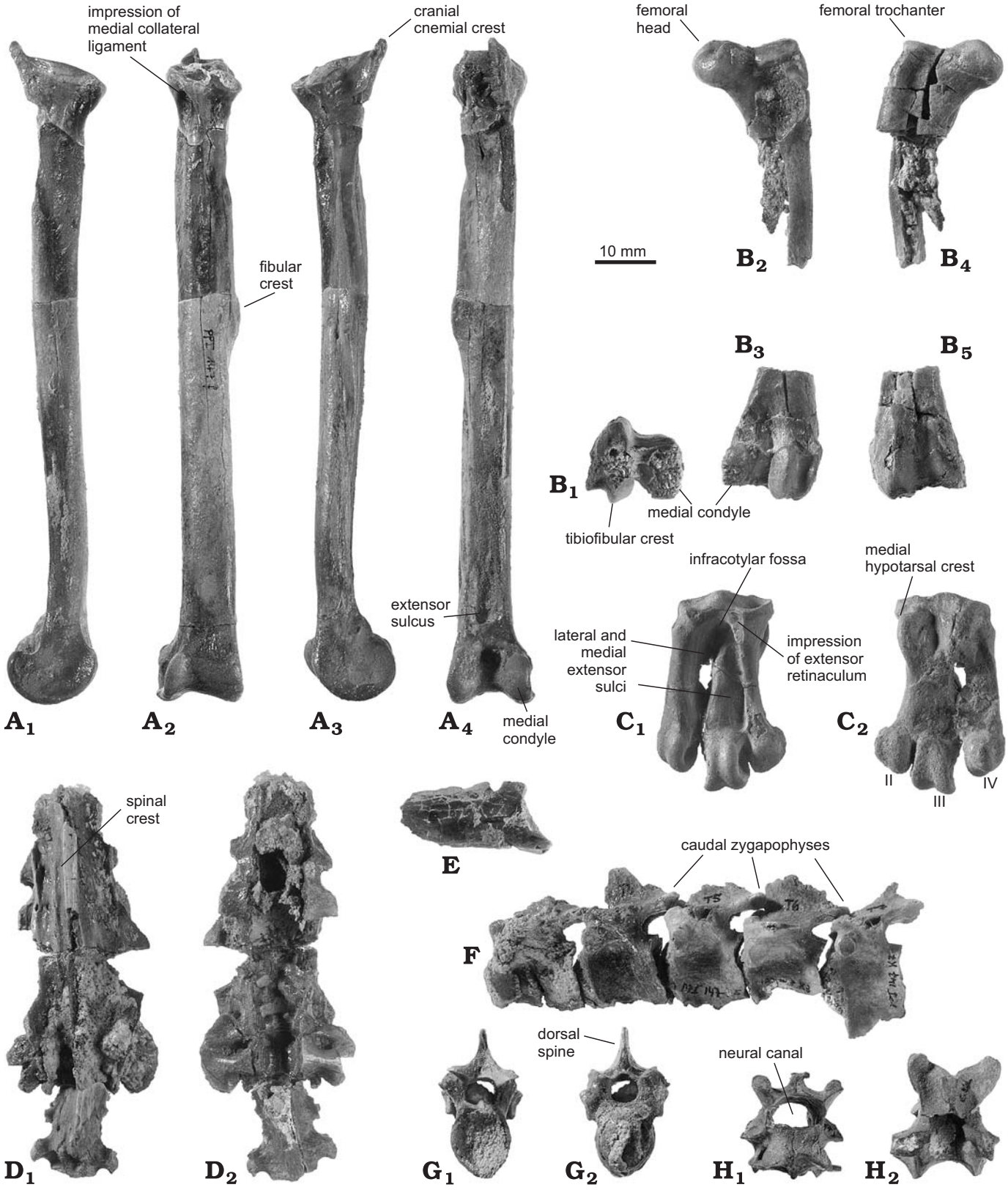

Fig. 3. Spheniscid penguin *Spheniscus muizoni* sp. nov. from Cerro la Bruja, latest middle/earliest late Miocene, Pisco Formation, Peru. **A**. Right tibiotarsus (MNHN PPI 147f), in medial (A_1), caudal (A_2), lateral (A_3), and cranial (A_4) views. **B**. Right femur (MNHN PPI 147e), distal end, distal view (B_1), proximal end, caudal view (B_2), distal end, caudal view (B_3), proximal end, cranial view (B_4), and distal end, cranial view (B_5). **C**. Right tarsometatarsus (MNHN PPI 147h), in dorsal (C_1) and plantar (C_2) views. **D**. Synsacrum (MNHN PPI 147l), in dorsal (D_1) and caudal (D_2) views. **E**. Pygostyl (MNHN PPI 152), in lateral view. **F**. Thoracic vertebrae T3-7? (MNHN PPI 147), in lateral view. **G**. Thoracic vertebra T4? (MNHN PPI 147), in caudal (G_1) and cranial (G_2) views. **H**. Cervical vertebra C12? (MNHN PPI 147), in caudal (H_1) and dorsal (H_2) views.

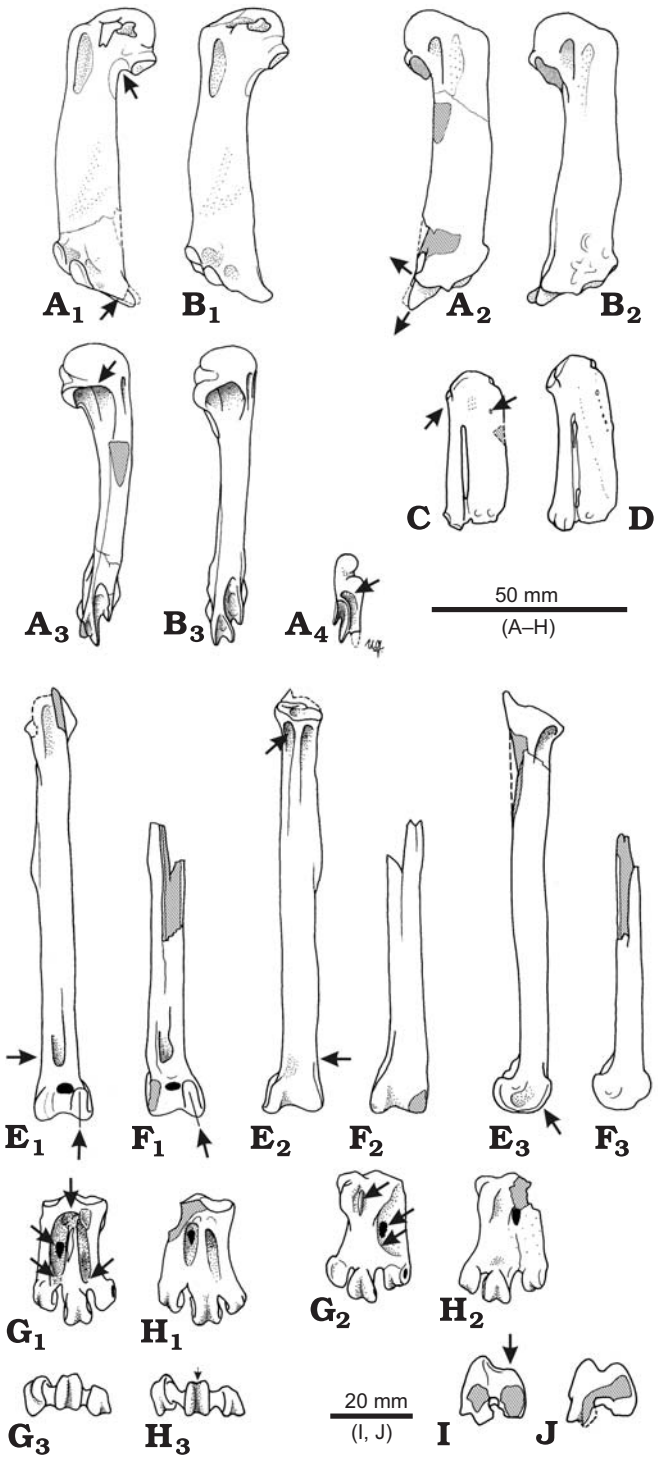

Fig. 4. Morphological differences between *Spheniscus muizoni* sp. nov. (**A**, **C**, **E**, **G**, **I**) and *Spheniscus chilensis* Emslie and Correa, 2003, paratype material from UF (**B**, **D**, **F**, **H**, **J**). **A**, **B**. Right humerus, in cranial (A_1, B_1), caudal (A_2, B_2), ventral (A_3, B_3), and distal (A_4) views. **C**, **D**. Right carpometacarpus, in dorsal view. **E**, **F**. Right tibiotarsus, in cranial (E_1, F_1), caudal (E_2, F_2), and medial (E_3, F_3) views. **G**, **H**. Right tarsometatarsus, in dorsal (G_1, H_1), plantar (G_2, H_2), and distal (G_3, H_3) views. **I**, **J**. Right femur, in distal view.

Humerus (Figs. 2C, 4A).—Left and right humeri (MNHN PPI 147c1+2) are preserved; the right one is quite complete; only the cranial surface of the proximal end and the caudal surface of the shaft are damaged and the cranial edge of the ventral epicondylus is broken off; the left humerus lacks the ventral epicondylus and the caudal and ventral walls of the pneumotricipital fossa are broken off. As is typical for fossil and extant species of *Spheniscus*, *S. muizoni* sp. nov. has a weakly proximally swollen humeral head, and also lacks the proximal notch between dorsal tubercle and humeral head (in caudal view; present in *Palaeospheniscus*); in both *S. muizoni* sp. nov. and *S. urbinai* the proximal outline from the head to the dorsal edge is less steep than in all compared extant species of *Spheniscus*. The pneumotricipital fossa is bipartite, with the cranial fossa being deep; this contrasts the genera *Paraptenodytes* and *Arthrodytes*, which fossa is non-bipartite (Simpson 1972: 18; Acosta Hospitaleche 2005: 407). The proximal border of the pneumotricipital fossa is in ventral view relatively straight and horizontal; this is also typical for the extant *Spheniscus* species, but contrasts the development of the fossil *Spheniscus* species, *S. urbinai* and *S. chilensis*, as well as *Dege hendeyi* and the extant penguins *Eudyptes chrysocome*, *E. chrysolophus*, and *Aptenodytes patagonicus*, where this border is concave proximally. Furthermore, in *S. muizoni* sp. nov. this margin, proximally bordering the pneumotricipital fossa, forms no ventrocaudally projecting lip (Fig. 5) separated from the head by an extended capital groove. As a result, the caudal surface of the proximal humerus end of *S. muizoni* sp. nov. is planar and shows no notch in dorsocaudal view. The lack of this ventrocaudally projecting lip is a common feature of *S. muizoni* sp. nov., *S. urbinai*, and *S. chilensis*, but contrasts all extant species of *Spheniscus* as well as those of *Pygoscelis.* The preaxial angle is weak (but stronger than in ?*Palaeospheniscus huxleyorum* and *D. hendeyi*) and situated about the mid-point of the shaft and thus is placed more proximally than in all other species of *Spheniscus*, *Palaeospheniscus*, *Eudyptes*, *Pygoscelis*, or *Aptenodytes.*

The ventral tubercle is strong and protruding, separated by a broad capital groove. *S. muizoni* sp. nov. differs from *S. chilensis* by a distinct concave indentation in the bicipital crest between ventral tubercle and shaft (Fig. $4A_1$, B_1). This indentation is also present only in *S. magellanicus*, hinted in *S. demersus* and slightly in *Pygoscelis adeliae*, but is lacking in *S. humboldti*, *Eudyptes*, *Py. papua*, *A. patagonicus*, and *Ps. huxleyorum*. In proximal view, the sulcus for the transversal ligament is short and deep; dorsal to it, a small, shallow dent is present like in *Spheniscus*, but which can vary in depth in other recent penguins and which can also form a short sulcus running distally, like in *A. patagonicus* or *Py. papua*. The fossa on the proximal caudal surface is as shallow as in all studied *Spheniscus* species, but is deeper when compared to *Eudyptes*, *Pygoscelis*, and *Aptenodytes*.

As is typical for *Spheniscus*, the line defined by ventral and dorsal condyle (in cranial/caudal view) is steeper than in *Eudyptes*, *Pygoscelis*, and *Aptenodytes.* On the ventral epicondylus, the tip of the caudal-most process, caudally bordering the humerodtricipital sulcus, is slightly rising upwards (ventroproximally), most notably its distal margin; this differs from the ventral orientation in *Spheniscus chilensis* (Fig. $4A_2$,

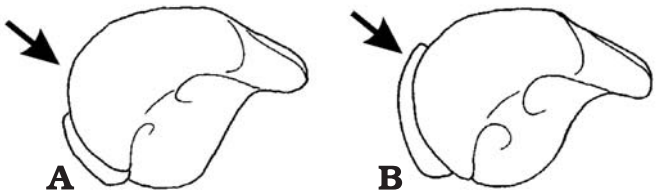

Fig. 5. Comparison of proximal humerus (in proximal view) of *Spheniscus muizoni* sp. nov. (**A**) and *Spheniscus humboldti* Meyen, 1834 (**B**), showing the difference in the development of the lip-like projection proximally bordering the fossa pneumotricipitalis. Not to scale.

B_2). The tip of the caudal-most process barely surpasses the ventral margin of the distal shaft (in cranial/caudal view), which corresponds to extant *Spheniscus* and *Eudyptes* species; it is longer and strongly surpassing in *Aptenodytes patagonicus*, moderately long in *Pygoscelis papua*, and shorter in *Inguza predemersus*. The middle process-like crest, caudally bordering the scapulotricipital sulcus, is slender, slightly pointed, and extends relatively far distoventrally; it is somewhat longer and oriented slightly more distally than in *S. chilensis* (Fig. $4A_2$, B_2). The cranial-most process-like crest, cranially bordering the scapulotricipital sulcus, is incomplete and missing its tip; however, the distal margin of the preserved part ends more proximally than that of the caudal process-like crest, unlike in *S. chilensis* (Fig. $4A_1$, B_1). In distal view, the dorsal end of the scapulotricipital sulcus is curved caudally (Figs. $2C_3$, $4A_4$).

Ulna (Fig. 2B).—Preserved are a complete left ulna (MNHN IPP 147d), belonging to the associated skeleton, and a slightly smaller fragmentary left ulna (MNHN IPP 149), with damaged proximal end and proximal caudal margin. They show no important differences from those of extant *Spheniscus*. The bone is flattened and expanded caudally into a crest-like flange; the ulna of *S. muizoni* sp. nov. is like the extant species of *Spheniscus* and like *Eudyptes*, relatively broader than the more slender ulnae of the representatives of *Pygoscelis* and *Aptenodytes*. In several extant penguin taxa the flange-like caudal margin shows in ventral or dorsal view in its distal half a slight indentation to which distally the bone becomes more slender; this recess is very weak in *S. muizoni* sp. nov. and situated at about the mid of the shaft, whereas it is situated more distally in *S. humboldti*, *S. demersus*, *Eudyptes chrysochome*, *E. chrysolophus*, *Py. adeliae*, *Py. papua*, and *A. patagonicus.* The dorsal side carries at least two rows of marked pits for the attachment of feather quills. This can also be observed in most specimens of extant *Spheniscus*, *Pygoscelis*, *Eudyptula*, and *Eudyptes*. The ventral side is marked by a longitudinal shallow concavity along the caudal margin of the flange-like caudal margin. The cranial side of the proximal end is flat; distoventrally to that, close to the cranial margin, there is a slender longitudinal brachialis impression. The distal shaft is dorsocranially swollen.

Radius (Fig. 2D).—An almost complete left radius (MNHN PPI 150), only missing the cranial distal edge, is present; it shows no important differences from the radii of the compared extant penguin species. In most of the latter the flange-like extended cranial crest ends proximally in a projecting peak. This is lacking in *A. patagonicus* and *Py. adeliae*, where the proximal end only forms an angle without projecting peak. This condition can also be observed in the radius of *S. muizoni* sp. nov., but it cannot be excluded that this character is liable to variation. As typical for penguins the dorsal side is marked by two furrows, one parallel to the cranial crest-like margin, the other one diagonal transversing the distal third of the radius from distocranially to proximocaudally.

Carpometacarpus (Figs. 2G, 4C).—An almost complete right carpometacarpus (MNHN PPI 154) is morphologically very similar to that of extant *Spheniscus*. Concerning limb bone length relations (Fig. 6), *S. muizoni* sp. nov. has a relatively short carpometacarpus, but which is relatively long for *S. chilensis*. The carpometacarpus of *S. muizoni* sp. nov. differs from *S. humboldti* and *S. demersus* by a short but distinct step between the proximal carpal trochlea and the extensor process of the alular metacarpal; such a step is low but present in *S. magellanicus*, and well developed in the compared species of *Eudyptes*, *Pygoscelis*, and *Aptenodytes*. The caudal margin of the minor metacarpal is less recessed below the carpal trochlea (Fig. 4C) in *S. muizoni* sp. nov. than in *S. chilensis*. In *S. muizoni* sp. nov. the line of fusion between alular digit and the major metacarpal is marked only by one foramen dorsally and none ventrally; thus, the fusion of these bones seems to be more progressive than in extant *Spheniscus* and also *S. chilensis*, which show at least two but often more foramina on both the ventral and dorsal side (Fig. 4C). The carpometacarpus is broadest at its distal shaft. The spatium is narrow and open, and shows no synchondroses, but which are present at least in both specimens of *S. chilensis* that were available for comparisons (UF 144110 figured in Emslie and Correa 2003: fig. 2C, and UF 144112). However, this character is more constant in extant species (own observation), but is observed to be variable, e.g., for *S. urbinai.*

Femur (Figs. 3B, 4I).—The right femur is represented by a proximal portion and a distal end (MNHN PPI 147e); in addition, there is a distal end of a right femur of another individual preserved (MNHN PPI 151). Both distal ends are slightly damaged. The femur corresponds well with those of the extant species of *Spheniscus*. The proximal portion of the femur is relatively straight, in contrast to that of *Py. papua* whose proximal half is curved medially. The femoral head and trochanter reach the same level in proximal direction as typical for all fossil and extant species of *Spheniscus*, but unlike in *Eudyptes chrysolophus*, *E. chrysochome*, *Py. papua*, *Py. adeliae*, and *A. patagonicus*, in which the trochanter surpasses the head more or less distinctly. The trochanteric crest projects cranially but not proximally on the trochanter. A large and deep obturator impression is laterally bordered by a prominent crest. The depth and size of this impression seem to vary within the compared extant species. The neck of the head is, in distal view,

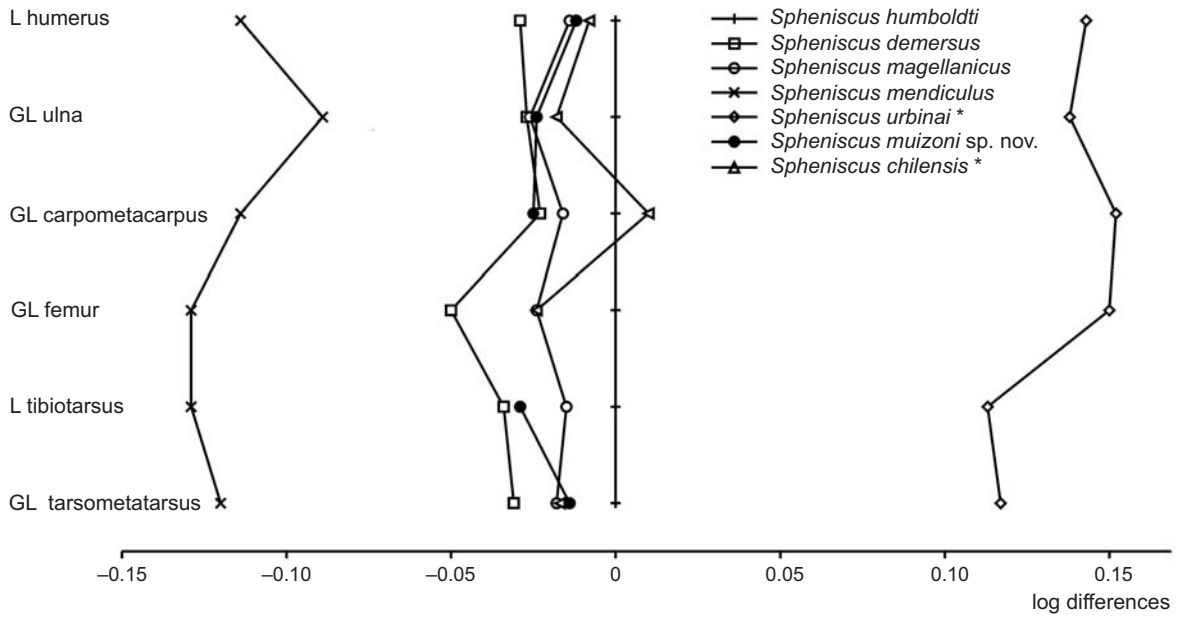

Fig. 6. Simpson's (1941) ratio-diagram of the main long bones of all extant and fossil *Spheniscus* species and some more fossil penguin species. The differences of the limb bone measurements, converted into logarithms, are shown in ratio to those of the chosen standard, *Spheniscus humboldti*. The horizontal distance between the points, marking the same bone elements of different taxa, is proportional to the ratio of their real dimensions. It is essentially: log (mean of measurement of compared taxon) – log (mean of measurement of standard taxon) = log (mean of measurement of compared taxon / mean of measurement of standard taxon). L, length; GL, greatest length. Fossil taxa are indicated by an asterisk.

slightly thinner than in all compared extant specimens. Characteristic for *S. muizoni* sp. nov. is the cranially very low, barely projecting medial condyle (in distal and medial view; Fig. 4I), lower than in the compared extant species of *Spheniscus* as well as in *S. chilensis* (Fig. 4J) and *S. urbinai*. As in extant and fossil *Spheniscus* species, the lateral condyle cranially reaches further proximally than the medial one, whereas the condyles reach about equally far proximally in most of the compared specimens of *Eudyptes*, *Pygoscelis*, and *Aptenodytes*. In distal view, the tibiofibular crest of the lateral condyle caudally projects relatively high and is sharp-crested; its medial flank is steep like in extant *Spheniscus*, but steeper compared to *Eudyptes*, *Pygocelis*, and *Aptenodytes* specimens. The sulcus of the fibular trochlea is relatively deep. There is a deep cranial impression for the attachment of the cruciate ligament in the intercondylar sulcus.

Tibiotarsus (Figs. 3A, 4E).—The right tibiotarsus is almost complete, only the proximal end of the lateral and cranial cnemial crest are somewhat damaged, the left tibiotarsus is represented by its proximal end, with also damaged crests (MNHN PPI 147f-1+2). The proximal end is caudally characterized by two fossae, separated by a longitudinal crest, which is relatively sharp-edged and proximally quite thin. The lateral longitudinal flexor fossa is also more or less developed in extant penguins; however, characteristic is the deep and distinct medial fossa (impression) of the collateral ligament (Fig. $4E_2$); it is mostly not or only very weakly developed in most compared extant species (weak in *S. magellanicus* and in one of the two compared specimens of *Py. papua*). Also characteristic is a distinct furrow along the lateral side of the distal shaft, starting on the caudal side distal to the fibular crest and turning to the laterocranial side in distal direction; this furrow is much weaker in all of the compared extant penguin specimens.

Remarkable is the straight distal end of the tibiotarsus of *S. muizoni* sp. nov., contrasting most extant and fossil penguins (*S. urbinai*, *Palaeospheniscus*), which distal end is bent medially (in cranial view). Furthermore, the medial condyle is vertical in *S. muizoni* sp. nov. and not laterally inclined and lacks a swollen tubercle for the retinaculum of the fibularis muscle forming the lateral bulge on the distal shaft (Fig. $4E_1$, E_2); instead of the latter there is only a very weak vertical line. In contrast, this lateral bulge is present in most extant *Spheniscus* species, *Pygoscelis*, *Eudyptes*, and *Aptenodytes*. Only *S. magellanicus* and *S. chilensis* also show a quite straight distal end of the tibiotarsus, provoked by very weak lateral tubercle for the retinaculum of the fibularis muscle, but differ by an inclined medial condyle (Fig. $4F_1$).

Unlike extant and other fossil penguin taxa, the distal end of the tibiotarsus of *S. muizoni* sp. nov. lacks the furrow between the tubercle for the retinaculum of the fibularis muscle and the extensor sulcus, and both the medial and lateral tuberosity for the extensor retinaculum on both sides of the extensor sulcus; the latter distinguishes *S. chilensis*, which has a distinct lateral tuberosity for the extensor retinaculum (Fig. $4E_1$, E_2, F_1, F_2). The medial border of the extensor sulcus is relatively thin and straight. Like other fossil and extant species of *Spheniscus*, *S. muizoni* sp. nov. lacks the craniolaterally protruding lip-like crest (tuberositas retinaculi extensoris medialis), but which is present in *Eudyptes* and also sometimes in *Pygoscelis* and *Aptenodytes.* The lateral condyle is sub-rounded, the medial one is more longer

craniocaudally; unlike in *S. chilensis* and *Eudyptes*, the distal margin of the medial condyle (in medial view) is not distally notched but round (Fig. $4E_3$, F_3). A weak tubercle is present proximal to the lateral condyle, which is more or less developed also in extant penguin species. A tiny foramen is situated lateral to this tubercle. It is present in most penguins (except *Aptenodytes patagonicus*), but its position varies from proximal to the tubercle in *S. humboldti* and *S. demersus*, to lateral of it in *S. magellanicus*, *Py. papua*, and *Py. adeliae*.

Fibula.—The fibula is represented by a proximal portion of a right specimen (MNHN PPI 147g). The proximal articular facet for the femur is slightly damaged but was craniocaudally concave. The medial articular facet for the tibia is flat. The fibula of *S. muizoni* sp. nov. is characterized by a distinct and very deep concavity on the caudal side, which is less deep or almost absent in the extant species. The proximal shaft of the fibula is laterally marked by a distinct furrow running obliquely from proximocranial to distocaudal. This furrow is very well developed and also present in all compared species but can vary intraspecifically.

Tarsometatarsus (Figs. 3C, 4G).—One complete right tarsometatarsus (MNHN PPI 147h) is present. Fig. 6 shows that the tarsometatarsus of *S. muizoni* sp. nov. is relatively long in comparison with most extant *Spheniscus* species. It is slender and extends especially distally.

The elongation index of *S. muizoni* sp. nov. (2.07) is higher than that of *S. urbinai* (1.7–1.95; see Table 2), below that of *Palaeospheniscus*, which is diagnostically about 2.2–2.4 (Simpson 1972: 8) and distinctly below that of *E. tonnii* (elongation index: 2.66, Acosta Hospitaleche et al. 2004: 235), but is in the range of that of *Paraptenodytes* (elongation index: 1.8–2.1). However, *Pa. robustus* and *Pa. antarcticus* are distinctly larger species. The elongation index of *S. chilensis* is not known, but its ratio of length/least breadth of shaft (length: 33.5 mm, least breadth of shaft: 16 mm, unpublished data provided by Steve Emslie) is 2.09, whereas that of *S. muizoni* sp. nov. is 2.24.

The extensor sulci in *S. muizoni* sp. nov. are long and deep, as in *Spheniscus*. In contrary, both sulci are shallower in *Eudyptes*, *Pygoscelis*, and *Aptenodytes* and in *Palaeospheniscus* (*Ps. patagonicus* and *Ps. bergi*) the medial sulcus is shallower. However, the medial sulcus of *S. muizoni* sp. nov. is in its distal part deeper than in extant species of *Spheniscus*. Emslie and Correa (2003) described the extensor sulci of *S. chilensis* as shallow below the proximal foramen; from own observations, I would surmise that they are deep proximally but shallow only in their distal half. However, this is different from *S. muizoni* sp. nov., in which the sulci are also deep distally (Fig. $4G_1$, H_1).

There are very probably two proximal vascular foramina, unlike in the smaller-sized species *E. tonnii* (Acosta Hospitaleche et al. 2004: 235) and *N. insolitus* (from the early Pliocene of Duinfontain, South Africa [Simpson 1979a]), which are characterized by only one foramen. In *S. chilensis* the medial proximal foramen of the tarsometatarsus is described as "…greatly reduced or absent…" (Emslie and Correa 2003: 313). In *S. muizoni* sp. nov. the lateral proximal vascular foramen is probably situated in the middle of the lateral dorsal extensor sulcus, but where the bone is damaged; the medial one is small, situated more proximally than the lateral one in the most proximomedial edge of the infracotylar fossa and opens plantarly on the medial surface of the hypotarsus. The arrangement of the proximal foramina corresponds more to that of *Spheniscus* than to any other extant genus, but the medial foramen is situated more proximal than in extant species. The position and size of these foramina also differs from *Inguza predemersus*.

The dorsal infracotylar fossa is very deep in that the proximal portion of the metatarsal III is distinctly lower than that of metatarsals II and IV. The proximal end of the metatarsal II dorsally carries a very pronounced impression of the extensor retinaculum (defining a distinct fossa) and a little distally to another small muscle or tendon scar; the arrangement and distinctiveness of these impressions and scars also corresponds mostly with the genus *Spheniscus*, whereas it is much weaker in *Eudyptes chrysolophus*, *E. chrysochome*, *Py. papua*, and *A. patagonicus*. The metatarsal III carries dorsally a long tuberosity for the attachment of the tibialis muscle.

The hypotarsus is relatively weak in comparison with extant *Spheniscus* species. The medial hypotarsal crest is relatively thin and oriented medioplantarly (not lateroplantarly as in *Palaeospheniscus*); in proximal view it is bent hook-like medially with a concave furrow along its medial side; laterally attached to it (along its distal half) is a second very weak crest. The lateral hypotarsal crest is very weak and hardly projecting; laterally it is limited by a ridge, which runs distally passing medially to the lateral proximal foramen. Lateral to the ridge, the plantar surface of the proximal shaft is concave.

The medial metatarsal (II) is more slender than the middle (III) and the lateral one (IV). In lateral view, a plantarly concave ridge borders the lateroplantar side of the metatarsal IV.

As typical for all extant and fossil *Spheniscus* species, the lateral intertrochlear incision is longer (deeper incised proximally) than the medial one (in dorsal view), whereas in *A. patagonicus*, *E. chrysochome*, and *Py. papua* they incise about the same length.

In *S. muizoni* sp. nov. as well as in all extant and fossil species of *Spheniscus*, the trochlea II and IV are of about equal length distally; this is different in extant *Eudyptes*, *Pygoscelis*, and *Aptenodytes* and fossil *Palaeospheniscus* (*Ps. patagonicus* and *Ps. bergi*), which trochlea VI is somewhat shorter than II.

Trochlea III is very robust and swollen dorsally. In distal view, trochlea III reaches dorsally at the same level as the lateral condyle of trochlea VI or slightly surpasses it (also in lateral view). *S. muizoni* sp. nov. shares this feature with *S. urbinai* (and with *E. chrysolophus*), but differs from *S. chilensis* and all extant species of *Spheniscus*, which trochlea IV dorsally surpasses the lateral condyle of trochlea III (Fig. $4G_3$, H_3). Additionally, the lateral bulge of trochlea IV is dorsoplantarly lengthened and clearly surpasses trochlea III

in plantar direction. The medial and lateral condyle of trochlea III are dorsally about the same level, whereas in extant *Spheniscus* species, the medial one is clearly surpassing the lateral one. In lateral view, the lateral condyle of trochlea IV is distally somewhat flattened and shorter than the medial one (like in *Pygoscelis papua* and *Aptenodytes*), unlike in extant *Spheniscus*. Trochlea II is oriented relatively obliquely, so that the medial fovea is apparent in dorsal view.

Sternum (Fig. 2E).—Only a small, cranial-most center portion of the sternum with both sulci for the coracoid articulation is present. The cranial spines (spina interna and externa) and the carina are broken off.

Cervical vertebrae (Fig. 3H).—The probable two caudal-most cervical vertebrae (C12, C13) are represented. C12 is quite complete, but lacking the transverse processes, of C13 only the body is preserved. Both vertebrae are strongly heterocoel and characterized by deep lateral dents on the lateral concavities of the body, as typical for these vertebrae positions. C12 has a short spinosus and ventral processes.

Thoracic vertebrae (Fig. 3F, G).—Seven thoracic vertebrae out of normally eight are preserved; they probably represent the cranial-most ones (T1–T7). All of them show the lateral depressions for the rib articulation. First and second vertebrae (T1, T2) are preserved fragmentary; T1 lacks the dorsal arc, T2 its caudal half. T3–T7 (Fig. 3F) are more complete, but lack all ventral or dorsal spines and the transverse processes; the cranial and caudal zygapophyses are mostly preserved. The first two vertebrae, even if fragmentary, show moderate heterocoel articulation facets, whereas the further five vertebrae are opisthocoel.

Synsacrum (Fig. 3D).—The synsacrum is represented by two fragments, a short portion of the cranial end and the rest of the fragmentary synsacrum, but both portions lack contact. The cranial portion is represented only by the laterally strongly flattened body with a worn convex cranial articular facet and ventrally forms a longitudinal crest. The larger caudal portion lacks the body of the synsacrum, thus the vertebral canal is open; additionally, both lateral edges of the synsacrum are badly damaged; in its cranial half the spinosus crest is preserved, which becomes higher in the cranial direction. The sinoid structure forming the iliosynsacral suture is only partly preserved by their caudal portions, which are laterally concave. The number of vertebrae involved in the synsacrum is not reconstructible.

Pygostyle (Fig. 3E).—About the cranial half of the pygostyle is preserved. It is laterally strongly flattened. The cranial articulation is oval and higher than broad. The basis of the pygostyle is damaged.

Estimating the living weight based on the relationship of the body mass of birds with some hindlimb measurements (circumference of the shafts of femur and tibiotarsus), a method presented by Campbell and Marcus (1992), the femur leads to a weight of about 3500 g, and the tibiotarsus to a weight of about 3800 g for *S. muizoni* sp. nov.; these calculations were made by considering penguins as swimmers (SW in Campbell and Marcus 1992). The estimated living weight of *S. muizoni* sp. nov. corresponds well with the body mass of *S. demersus*, 3310 g for males and 2960 g for females, but is somewhat smaller than that for *S. magellanicus* (4500 g) and distinctly smaller than that for *S. humboldti* (4500 g), but is larger than that for *S. mendiculus* (2500 g; body masses by Dunning 1993).

Stratigraphic and geographic distribution.—Only known from the latest middle or earliest late Miocene of the type locality Cerro la Bruja.

Conclusion

Detailed comparisons with extant and fossil species of *Spheniscus* suggest that the available postcranial bones of *S. muizoni* sp. nov. morphologically correspond best with those of *S. urbinai*, aside from that the latter is distinctly larger. Some shared features are found to be exclusive for these two species within *Spheniscus*, such as the lack of a ventrocaudally projecting lip proximally bordering the pneumotricipital fossa on the humerus, or a tarsometatarsus which trochlea III is dorsally at about the same level as the lateral condyle of trochlea VI or slightly surpasses it. Although of almost identical size, *S. muizoni* sp. nov. can be distinguished by several osteological features from *S. chilensis*, such as the limb bone proportions of the carpometacarpus (Fig. 6) and morphological differences at the humerus, carpometacarpus, femur, tibiotarsus, and tarsometatarsus. Based on the morphological similarity of *S. muizoni* sp. nov. and *S. urbinai* and their stratigraphical succession within the Pisco Formation, it can be supposed that the first gave directly rise at least to the latter.

S. muizoni sp. nov. is the only known penguin species from the Cerro la Bruja locality and is unknown from any older or younger deposit in or outside the Pisco Formation. As penguins are shorebirds—breeding on land (or ice) and feeding in fairly adjacent marine waters (del Hoyo et al. 1992), the penguin fossils complement the exclusively marine vertebrate fauna represented at Cerro la Bruja, comprising fossil taxa of marine fishes (Teleostei) and sharks (Selachii), a turtle and a crocodile, different marine mammals such as fossil odontocetes (Kentriodontidae, Pontoporiidae), mysticetes (Cetotheriidae, Balaenopteridae), pinnipeds (Phocidae), and a boobie (Aves, Sulidae; Muizon 1988: table 1).

To date, all fossil penguins reported from the different levels of the Pisco Formation belong to the extant genus *Spheniscus*. The today living species of *Spheniscus* include: *S. mendiculus* (Galapagos), *S. humboldti* (coast of Peru and Chile), *S. magellanicus* (coast of Chile and Argentina, Islas Malvinas or Falkland Islands), and *S. demersus* (coast of South Africa and Namibia; del Hoyo et al. 1992).

However, *S. muizoni* sp. nov. from the latest middle/earliest late Miocene of Cerro la Bruja is not only the most ancient

penguin species in the Pisco Formation, but also the stratigraphically oldest record for the extant genus *Spheniscus* in general.

The fossil record indicates a faunal change of *Spheniscus* species within the stratigraphically older sequence of the Pisco Formation. *S. muizoni* sp. nov., exclusive in the oldest deposits (latest middle/earliest late Miocene, 13–11 Ma) is replaced by the persistant *S. urbinai*, existing from the late Miocene to the early Pliocene (9 to 3.5 Ma) deposits (*S. megaramphus* is only known from a 6 Ma old locality). This replacement might be linked to changes of the climatic conditions at the Pacific coast of South America during the latest middle Miocene. Tsuchi (2002: 269) dated a short warm episode in between cool episodes of the surface marine climate of the latest middle Miocene at ca. 11.5 Ma, which is supported by deposits rich in warm water planktonic foraminifera in northern Chile. Extant penguins (on a species level) require a relatively stable water temperature (del Hoyo et al. 1992: 144) and change of water temperature (e.g., as in the phenomenon known as El Niño) is known to have far reaching effects on the Humboldt and Galapagos Penguin. It is not known yet, if there is a faunal consequence also within some other fossil vertebrate groups represented in Cerro la Bruja and younger localities in the Pisco Formation because the vertebrate fauna of Cerro la Bruja has not been studied in detail as yet.

Apart from *Spheniscus*, there is only very scanty penguin material known from other Peruvian localities, which is described as *Palaeospheniscus* sp. and Spheniscidae indet. (Acosta Hospitaleche and Stucchi 2005). However, the latter comes from deposits older than the Pisco Formation, the lower middle Miocene Chilcatay Formation and the upper Eocene–lower Oligocene Otuma Formation, respectively.

Outside the Pisco Formation, fossil representatives of *Spheniscus* have been reported only from Chile: *S. chilensis* from the late Pliocene and *Spheniscus* sp. from the late Miocene–early Pliocene. There was only one report on a fossil *Spheniscus* outside of South America, *S. predemersus* Simpson, 1971 described from South Africa. This species was, however, later referred by Simpson (1975b) to the new genus *Inguza*.

Thus, the fossil record of *Spheniscus* is restricted to the latest middle/earliest late Miocene to the late Pliocene of South America, more precise to the Pacific coast of South America (Peru and Chile). The modern distribution of *Spheniscus* correlates with cold marine currents—the west-east directed Circumpolar Antarctic Current and their northern upturns along the west-coasts of South America (Humboldt Current) and southern Africa (Benguela Current). However, the restriction of the Mio-Pliocene record of *Spheniscus* to the Pacific coast of South America was not due to a geographic barrier, as the Drake passage was already open by the late middle Eocene around 40 Ma ago (Scher and Martin 2006). However, no record of *Spheniscus* is known along the Atlantic coasts of South America or southern Africa during the Neogene. However, the presence of this genus cannot be ruled out if their restriction to the Pacific coast during the Neogene is linked to other ecological or alimentary factors—perhaps interrelated to the still open Panama Isthmus (closure starts during the early Pliocene, about 4–3 Ma, Kameo and Sato 2000) and thus corresponding marine currents, which might had an effect on the distribution of potential prey. In all extant *Spheniscus* species pelagic school fish (mostly anchovies) is the dominant prey; cephalopods and crustaceans are subordinate (del Hoyo et al. 1992). Because the skull of *S. muizoni* sp. nov. is lacking, no information is available on the shape of the bill, which varies at least in some extant penguin genera and their preferred diet. Neither fossil nor extant *Spheniscus* species show any obvious interrelation of body size and latitude of their habitat.

Acknowledgements

This study was conducted at UBCL. I warmly thank Cécile Mourer-Chauviré (UCBL) for her general assistance with this study, her helpful comments of the manuscript and her hospitality during my fellowship in Lyon. I am indebted to Serge Legendre and Christophe Lécuyer (both UCBL) for their assistance and their financial support, and Christian de Muizon (MNHN) for placing the studied material at my disposal. David Steadman (FMNH) made paratype material of *Spheniscus chilensis* available. Steve Emslie (University of North Carolina, Wilmington, USA) and Kenneth Campbell (LACM) kindly provided unpublished measurement data for *S. chilensis* and for *S. mendiculus*, respectively. Photos were made by Noël Podevigne (UCBL). I thank Laura L. Schulz (Tracy, CA, USA) for improving the English and the reviewers Carolina Acosta-Hospitaleche (Museo de La Plata, Ciudad de La Plata, Argentina) and Steve Emslie for their helpful comments on the manuscript. I am grateful to the Alexander von Humboldt Foundation, Germany, for support of this research through a fellowship in the Feodor-Lynen-Program. Financial support by the UCBL and the Centre National de la Recherche Scientifique (CNRS) was appreciated.

References

Acosta Hospitaleche, C. 2003. *Paraptenodytes antarcticus* (Aves: Sphenisciformes) en la Formación Puerto Madryn (Mioceno tardío temprano), provincia de Chubut, Argentina. *Revista Española de Paleontología* 18: 179–183.

Acosta Hospitaleche, C. 2005. Systematic revision of *Arthrodytes* Ameghino, 1905 (Aves, Spheniscidae) and its assignment to the Paraptenodytinae. *Neues Jahrbuch für Geologie und Paläontologie, Monatshefte* 7: 404–414.

Acosta Hospitaleche, C. and Canto, J. 2005. Primer registro de cráneos de *Palaeospheniscus* (Aves, Spheniscidae), procedentes de la Formación Bahía Inglesa (Mioceno Medio-Tardío), Chile. *Revista Chilena de Historia Natural* 78: 489–495.

Acosta Hospitaleche, C. and Stucchi, M. 2005. Nuevos restos terciarios de Spheniscidae (Aves, Sphenisciformes) procedentes de la costa del Perú. *Revista Española de Paleontología* 20: 1–5.

Acosta Hospitaleche, C. and Tambussi, C. 2004a. Fossil penguins from South America. *Abstracts Book, Vth International Penguin Conference, Ushuaia, Argentina*, 48.

Acosta Hospitaleche, C. and Tambussi, C. 2004b. Systematic revision of South American fossil penguins (Sphenisciformes). *6th International Meeting of the Society of Avian Paleontology and Evolution, Quillan, France*, 3.

Acosta Hospitaleche, C., Chávez, M., and Fritis, O. 2006. Pinguinos fósiles (*Pygoscelis calderensis* sp. nov.) en la Formación Bahía Inglesa (Mioceno Medio-Plioceno), Chile. *Revista Geológica de Chile* 33: 327–338.

Acosta Hospitaleche, C., Tambussi, C., and Canto, J. 2005. Catálogo comentado de los pingüinos (Aves, Sphenisciformes) fósiles del Museo Nacional de Historia Natural de Santiago, Chile. *Boletín del Museo Nacional de Historia Natural de Santiago* 54: 141–151.

Acosta Hospitaleche, C., Tambussi, C., and Cozzuol, M. 2004. *Eretiscus tonnii* Simpson 1981 (Aves, Sphenisciformes): materiales adicionales, status taxonómico y distribución geográfica. *Revista del Museo Argentino de Ciencias Naturales* 6 (2): 632–637.

Acosta Hospitaleche, C., Tambussi, C., Donato, M., and Cozzuol, M. 2007. A new Miocene penguin from Patagonia and its phylogenetic relationships. *Acta Palaeontologica Polonica* 52: 299–314.

Ameghino, F. 1891. Enumeración de las aves fósiles de la República Argentina. *Revista Argentina de Historia Natural* 1: 441–453.

Ameghino, F. 1895. Sur les oiseaux fossiles de Patagonie. *Boletín del Instituto Geografia Argentina* 15: 501–602.

Ameghino, F. 1899. *Sinopsis geológico-paleontológica. Suplemento (Adiciones y correcciones)*, 1–13. La Libertad, La Plata.

Ameghino, F. 1901. L'âge des formations sédimentaires de Patagonie. *Anales de la Sociedad Científica Argentina* 51: 20–39, 65–91.

Ameghino, F. 1905. Enumeración de los impennes fósiles de Patagonia y de la Isla Seymour. *Anales del Museo Nacional de Buenos Aires* 3 (6): 97–167.

Ameghino, F. 1920. Sur les édentés fossiles de l'Argentine. Examen critique, révision et correction de l'ouvrage de la M.R. Lydekker. *Obras Completas y Correspondencia Cientifica* 11: 447–909.

Baumel, J.J., King, A.S., Breazile, J.E., Evans, H.E., and Van den Berge, J.C. 1993. Handbook of avian anatomy: Nomina Anatomica Avium. *Publications of the Nuttall Ornithological Club* 23: 1–779.

Bonaparte, C.L. 1831. Saggio di una distribuzione metodica degli animali vertebrati. *Giournale Arcadico di Science Lettere ed Arti* 52: 155–189.

Campbell, K.E. Jr. and Marcus, L. 1992. The relationship of hindlimb bone dimensions to body weight in birds. *In*: K.E. Campbell Jr. (ed.), Papers in Avian Paleontology—Honoring Pierce Brodkorb. *Natural History Museum Los Angeles County, Science Series* 36: 395–412.

Cheneval, J. 1993. L'avifaune Mio-Pliocène de la formation Pisco (Pérou). Étude préliminaire. *In*: M. Gayet (ed.), Paléontologie et stratigraphie d'Amérique latine. Table ronde européenne (Lyon 1992). *Documents des Laboratoires de Géologie Lyon* 125: 85–95.

del Hoyo J., Elliott, A., and Sargatal, J. (eds.) 1992. *Handbook of the Birds of the World 1*. 696 pp. Lynx Edicions, Barcelona.

Driesch, A. von den 1976. *Das Vermessen von Tierknochen aus vor- und frühgeschichtlichen Siedlungen*. 114 pp. Institut für Paläoanatomie, Domestikationsforschung und Geschichte der Tiermedizin der Universität München, Munich.

Dunning, J.B. Jr. (ed.) 1993. *CRC Handbook of Avian Body Masses*. 371 pp. CRC Press Boca, Raton.

Emslie, S.D. and Correa, C.G. 2003. A new species of penguin (Spheniscidae: *Spheniscus*) and other birds from the late Pliocene of Chile. *Proceedings of the Biological Society of Washington* 116: 308–316.

Forster, J.R. 1781. Historia aptenodytae. Generis avivm orbi avstrali proprii. *Commentationes Societatis Regiae Scientiarum Gottingensis* 3: 121–148.

Kameo, K. and Sato, T. 2000. Biogeography of neogene calcareous nannofossils in the Caribbean and eastern equatorial Pacific—floral respons to the emergence of the Isthmus of Panama. *Marine Micropaleontology* 39: 201–218.

Linnaeus, C. 1758. *Systema naturae per regna tria naturae, secundum classes, ordines, genera, species, cum characteribus, differentiis, synonymis, locis. Tomus I. Editio decima, reformata*. 824 pp. Laurentius Salvius, Stockholm.

McDonald, G. and Muizon, C. de 2002. The cranial anatomy of *Thalassocnus* (Xenarthra, Mammalia), a derived nothothere from the Neogene of the Pisco Formation (Peru). *Journal of Vertebrate Paleontology* 22: 349–365.

Meyen, F.J.F. 1834. Beiträge zur Zoologie, gesammelt auf einer Reise um die Erde. 4. Abhandlung. *Novorum Actorum Academiae Caesareae Leopoldino-Carolinae Naturae Curiosorum* 16 (Supplement 1): 1–312.

Moehring, P.H.G. 1758. *Avium genera* [Latin MS in 1752, 58 pp. Bremen]. Published Dutch translation: C. Nozeman and A. Vosmaer (eds.) 1758. *Geslachten der Vogelen*. 97 pp. Pieter Meijer, Amsterdam.

Moreno, F.P. and Mercerat, A. 1891. Catálogo de los pájaros fósiles de la República Argentina. *Anales del Museo de La Plata (Paleontología Argentinia)* 1: 8–71.

Muizon, C. de 1984. Les vertébrés fossiles de la formation Pisco (Pérou). II – Les odontocètes (Cetacea, Mammalia) du Pliocène inférieur de Sud-Sacaco. *Travaux de l'Institut Français d'Études Andines* 27: 1–188.

Muizon, C. de 1988. Les vertébrés fossiles de la formation Pisco (Pérou). III – Les odontocètes (Cetacea, Mammalia) du Miocène. *Travaux de l' Institut Français d'Études Andines* 42: 1–244.

Muizon, C. de and DeVries, T.J. 1985. Geology and paleontology of late Cenozoic marine deposits in the Sacaco area (Peru). *Geologische Rundschau* 74: 547–563.

Muizon, C. de, McDonald, G., Salas, R., and Urbina, M. 2003. A new early species of the aquatic sloth *Thalassocnus* (Mammalia, Xenarthra) from the Late Miocene of Peru. *Journal of Vertebrate Paleontology* 23: 886–894.

Noriega, G. and Tambussi, C. 1989. Un Spheniscidae (Aves, Sphenisciformes) del Mioceno Tardio de la costa sur de Peru. VII Jornadas Argentinas Paleontologá Vertebrados. Abstract. *Ameghiniana* 26 (3–4): 247.

Olson, S.L. 1985. An early Pliocene marine avifauna from Duinefontein, Cape Province, South Africa. *Annals of the South African Museum* 95 (4): 147–164.

Scher, H.D and Martin, E.E. 2006. Timing and climatic consequences of the opening of Drake passage. *Science* 312: 428–430.

Sharpe, R.B. 1891. A review of recent attempts to classify birds. *Proceedings of the Second International Ornithological Congress* 2: 90. Budapest.

Simpson, G.G. 1941. Large Pleistocene felines of North America. *American Museum Novitates* 1136: 1–27.

Simpson, G.G. 1946. Fossil penguins. *Bulletin of the American Museum of Natural History* 87: 1–99.

Simpson, G.G. 1970. Miocene penguins from Victoria, Australia, and Chubut, Argentina. *Memoirs of the National Museum of Victoria* 31: 17–24.

Simpson, G.G. 1971. Fossil penguin from the Late Cenozoic of South Africa. *Science* 171: 1144–1145.

Simpson, G.G. 1972. Conspectus of Patagonian fossil penguins. *American Museum Novitates* 2488: 1–37.

Simpson, G.G. 1973. Tertiary penguins (Sphenisciformes, Spheniscidae) from Ysterplaats, Cape Town, South Africa. *South African Journal of Sciences* 69: 342–344.

Simpson, G.G. 1975a. Fossil penguins. *In*: B. Stonehouse (ed.), *The Biology of Penguins*, 19–41. University Park Press, Baltimore.

Simpson, G.G. 1975b. Notes on variation in pinguins and on fossil penguins from the Pliocene of Langebaanweg, Cape Province, South Africa. *Annals of the South African Museum* 69 (4): 59–72.

Simpson, G.G. 1979a. Tertiary penguins from the Duinefontein, Cape Province, South Africa. *Annals of the South African Museum* 79 (1): 1–7.

Simpson, G.G. 1979b. A new genus of Late Tertiary penguin from Langebaanweg, South Africa. *Annals of the South African Museum* 78 (1): 1–9.

Simpson, G.G. 1981. Notes on some fossil penguins, including new genus from Patagonia. *Ameghiniana* 18: 266–272.

Stephan, B. 1979. Vergleichende Osteologie der Pinguine. *Mitteilungen aus dem Zoologischen Museum in Berlin* 55 (3): 1–98.

Stucchi, M. 2002. Una nueva especie de *Spheniscus* (Aves: Spheniscidae) de la Formatión Pisco, Perú. *Boletín de la Sociedad Geológica del Perú* 94: 17–24.

Stucchi, M., Urbina, M., and Giraldo, A. 2003. Una nueva specie de Spheniscidae del Mioceno Tardío de la Formacíon Pisco, Perú. *Bulletin de l'Institut Français d'Études Andines* 32 (2): 361–375.

Sundevall, C.J. 1871. On birds from the Galapagos Islands. *Proceedings of the Zoological Society of London* 1871: 124–129.

Tsuchi, R. 2002. Neogene evolution of surface marine climate in the Pacific and notes on related events. *Revista Mexicana de Ciencias Geológicas* 19 (3): 260–270.

Walsh, S.A. and Hume, J.P. 2001. A new Neogene marine avian assemblage from north-central Chile. *Journal of Vertebrate Paleontology* 21: 484–491.

Walsh, S.A. and Suárez, M.E. 2006. New penguin remains from the Pliocene of Northern Chile. *Historical Biology* 18: 115–126.